RSC Advances

ROYAL SOCIETY OF CHEMISTRY

www.rsc.org/advances

RSC Advances

Paper

In-situ polymerization of liquid-crystalline thin films of electron-transporting perylene tetracarboxylic bisimide bearing cyclotetrasiloxane rings

Received 00th January 20xx,
Accepted 00th January 20xx

DOI: 10.1039/x0xx00000x

www.rsc.org/

Kaede Takenami,[a] Shinobu Uemura,[a] and Masahiro Funahashi*[a]

A perylene tetracarboxylic bisimide (PTCBI) derivative bearing four cyclotetrasiloxane rings that forms a columnar phase at room temperature despite the presence of the bulky cyclotetrasiloxane rings was prepared. The electron mobility in the columnar phase of this PTCBI derivative at room temperature is 0.12 $cm^2V^{-1}s^{-1}$, which is comparable to those of molecular crystals. The PTCBI derivative is soluble in various organic solvents and liquid crystalline thin films were successfully produced by a spin-coating method. The spin-coated films were insolubilized upon exposure to trifluoromethanesulfonic acid vapor. The columnar structure in the LC phase was retained during polymerization. Using a friction transfer method, macroscopically aligned LC thin films were produced and the optical anisotropy was retained after polymerization.

Introduction

The production of organic semiconductors via solution processes has recently been extensively studied from the viewpoint of practical device fabrication.[1a-c] Low molecular weight materials bearing bulky substitutents[1d] and conjugated polymers[1e] are important categories of these materials. Crosslinked thin films of organic semiconductors are effective for the production of multilayer structures by solution processes, as well as for production of self-standing films and stabilization of electronic devices.[2] For fabrication of practical devices, the flexibility of these thin films should be retained during the insolubilization process.

Liquid-crystalline (LC) semiconductors are solution-processable and can be applied to flexible electronic devices.[3] Electronic charge carrier transport in LC semiconductors in the columnar[4] and smectic phases has been confirmed,[5] and electroluminescence (EL) devices emitting linearly polarized light,[6] field-effect transistors,[7] and solar cells[8] using solution processable LC semiconductors have been developed. LC semiconductors offer the possibility for production of macroscopically aligned thin films[6b,7c-d] and flexible devices as advantages that are not offered by crystalline organic semiconductors.[7f]

Nanosegregation of molecules consisting of incompatible parts is an effective approach for constructing nanostructures in LC phases.[9] The LC molecules bearing π-conjugated units can be organized into LC phases to create flexible multi-functional electronic materials.[10] Recently, we reported nanosegregated LC semiconductors based on a perylene tetracarboxylic bisimide (PTCBI) core bearing oligosiloxane moieties.[11] These compounds form columnar phases at room temperature and exhibit high solubility in organic solvents. In the LC phases of these compounds, the formation of columnar and layer structures is promoted by nanosegregation between the liquid-like oligosiloxane moieties and rigid π-conjugated systems. In the columnar phases of the PTCBI derivatives, one-dimensional columnar aggregates of π-conjugated cores, in which efficient electron transport is achieved, are surrounded by a liquid-like mantle consisting of oligosiloxane moieties.

In general, it is not easy to produce macroscopically aligned thin films of LC polymers by solution processes. *In-situ* photopolymerization of nematic LC semiconductors in the thin film state has been investigated by O'Neill and Kelly.[12] They produced uniaxially aligned nematic thin films using LC fluorene derivatives bearing polymerizable 1,4-pentadiene moieties by photopolymerization. The photopolymerized thin films were applied to EL devices emitting linearly polarized light. The hole mobilities of the films were of the order of 10^{-4} $cm^2V^{-1}s^{-1}$.

Higher carrier mobility is expected in smectic and columnar phases.[3] *In-situ* polymerization in columnar or ordered smectic LC phases has been attempted by a few groups.[13-14] However, production of macroscopically aligned flexible thin films exhibiting high carrier mobility has been unsuccessful.

In this study, we present a novel *in-situ* acid-vapor-catalyzed polymerization method to produce uniaxially aligned thin films of the columnar LC semiconductor by the formation of an inorganic/organic hybrid network with an element-block structure.[15] We synthesized LC perylene tetracarboxylic bisimide derivatives **1** and **2** bearing polymerizable cyclotetrasiloxane moieties. These species form columnar phases at

[a]*Department of Advanced Materials Science, Faculty of Engineering, Kagawa University, 2217-20 Hayashi-cho, Takamatsu, Kagawa 761-0396 Japan. Fax: (+81)-87-864-2411; Tel: (+81)-87-864-2411; E-mail: m-funa@eng.kagawa-u.ac.jp*†
Electronic Supplementary Information (ESI) available: [Synthetic procedures and spectral data of the compounds]. See DOI: 10.1039/x0xx00000x

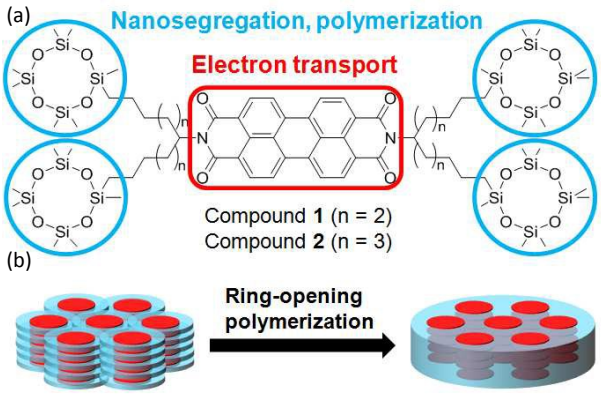

Figure 1 (a) Molecular structures of compounds **1** and **2** and (b) schematic illustration of ring-opening polymerization in the columnar phase.

room temperature, as shown in Figure 1(a), and exhibit high electron mobility exceeding 1×10^{-1} $cm^2V^{-1}s^{-1}$ at room temperature, in spite of the bulky cyclotetrasiloxane rings. Moreover, they are soluble in various organic solvents and LC thin films formed by a spin-coating method, in which the columnar axes are aligned perpendicular to the surface of the substrates. By exposing the LC thin films to trifluoromethane sulfonic acid vapor, insolubilized thin films are formed through acid-catalyzed ring-opening polymerization. By using a friction transfer method,[16] macroscopically uniaxial alignment of the columnar aggregates is achieved. The molecular aggregation states in the columnar phase and the photoconductivity are retained during the polymerization process. The polymerized LC thin films form self-standing films that can be bent.

As illustrated in Figure 1(b), in the columnar phases of compounds **1** and **2**, nanosegregation between the π-conjugated cores and the cyclotetrasiloxane rings is a driving force for formation of the LC structures. Nanosegregation causes the cyclotetrasiloxane rings to interdigitate to form a core-shell structure, in which electron-transporting one-dimensional stacks are surrounded by insulating mantles consisting of cyclotetrasiloxane rings. Upon exposure to the acid vapor, ring-opening polymerization occurs only in the mantle, while retaining the structures of the central electroactive stacks.

Experimental

Characterization of mesophases

The mesomorphic properties of the PTCBI derivatives were studied by differential scanning calorimetry (DSC), polarizing optical microscopy, and X-ray diffraction. A polarizing optical microscope (Olympus DP70) equipped with a hand-made hot stage was used for visual observation of the optical textures. Differential scanning calorimetry (DSC) measurements were conducted with a NETZSCH DSC 204 Phoenix instrument. X-ray diffraction (XRD) measurements were carried out on a Rigaku Rapid II diffractometer with the use of Ni-filtered CuKα radiation.

Measurement of carrier mobility in the LC phases

The electron mobilities were measured by the time-of-flight (TOF) method. A liquid crystal cell was fabricated by combining the two ITO-coated glass plates. The surface of the ITO-coated substrates was cleaned by UV-O_3 treatment. The cell was placed on a hot stage and heated at 140 °C. Compound **1** was melted and capillary-filled into the cell. The cell was cooled to 130 °C at a rate of 0.1 °C /min. Dark domains in which columnar stacks were homeotropically aligned were observed under an optical microscope. The liquid crystal cell was placed on a hot stage of the TOF setup. DC voltage was applied to the cell using an electrometer (ADC R8252) and a pulse laser was used to irradiate the cell. The third harmonic of a Nd:YAG laser (Continuum MiniLite II, wavelength = 356 nm, pulse duration: 2 ns) was used as the excitation source, and induced displacement currents were recorded by a digital oscilloscope (Tektronics TDS 3044B) through a serial resistor.

Synthesis of Materials

All ^{1}H and ^{13}CNMR spectra were recorded on a Varian UNITY INOVA400NB spectrometer. FT-IR measurements were conducted on a JASCO FT/IR-660 Plus spectrometer. Perylene tetracarboxylic acid anhydride and the Karstedt catalyst were purchased from Tokyo Chemical Industry and Gelest Inc., respectively. Zinc acetate, quinoline, and toluene (which were commercially available from Wako Pure Chemical Industries) were used without purification. Silica gel was purchased from Kanto Chemicals.

LC PTCBI bisimide derivatives **1-2** bearing heptamethylcyclotetrasiloxane moieties were synthesized according to the procedure reported previously.[11d] The treatment of perylene tetracarboxylic anhydride with alkenylamine in the presence of zinc acetate in quinoline at 150 ºC produced PTCBI derivatives **3** and **4** bearing alkenyl chains. Compounds **3-4** were reacted with 1,3,3,5,5,7,7-heptamethylcyclotetrasiloxane in the presence of the Karstedt catalyst (bisdimethylvinylsiloxane platinum (0)), thereby producing compounds **1** and **2**. Products **1** and **2** were purified repeatedly by silica gel column chromatography and reprecipitation in methanol.

We previously reported the synthesis, mesomorphic property, and electron transport of compound **2**.[11d] Because of isomerization of the cyclotetrasiloxane rings, the crude product of compounds **1** and **2** contain trace amounts of isomeric

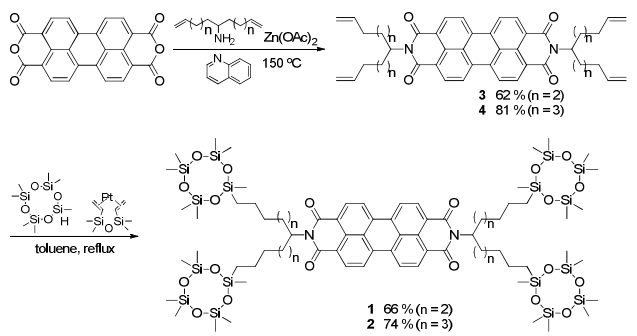

Scheme 1 Synthetic route of LC compounds **1-2**

impurities. These impurities could be removed from the crude products by repeated column chromatographic purification using *n*-hexane as the eluent. After removal of the isomeric impurity, the clearing point of compound **2** increased from 80 ºC to 84 ºC, although no crystallization was observed on cooling and heating.

Production of thin films and their *in-situ* polymerization

A toluene solution (10 wt %) of compound **2** was spin-coated on glass substrates. Spin-coating was performed at a rotation speed of 2000 rpm for 30 s and 3000 rpm for 30 s. The deposited films were dried under vacuum for one day.

The thin film deposited on the glass substrate was placed in a Petri dish. A small glass dish containing several drops of trifluoromethane sulfonic acid was also placed in the dish which was capped with another Petri dish. The dish was placed in an oven set at 80 ºC and kept for 1 h. After exposure to the acid vapor, the thin film was immersed in a toluene solution of triethylamine for 15 min in order to remove absorbed acid from the polymerized thin film.

The thickness of the deposited thin films was determined by using a DEKTAK 6 instrument. UV-Vis absorption spectra were acquired by using a JASCO Ubest V-530iRM instrument. The surface morphology of the thin films was observed with a Nanoscope IV MultiMode atomic force microscope (AFM) (Veeco, Present: Bruker AXS) operating in tapping mode™ in air. Silicon cantilevers (OMCL-AC240TS) with an apparent resonance frequency of 70 kHz were used.

Results and discussion

Mesomorphic property of compounds 1-2

Compounds **1**-**2** formed columnar phases at room temperature and these columnar phases were retained when the samples were cooled to -100 ºC.

Figures 2(a)–(d) display polarizing optical micrographs of the columnar phases of compounds **1** and **2**. Compound **1** exhibited a supercooled mesophase at room temperature, as shown in Figure 2(a). However, the supercooled state was not stable at room temperature. Partial crystallization occurred when the sample was left at room temperature for 1 h (Figure 2 (b)). The mesophase of compound **1** was miscible with the columnar phase of compound **2**, and the LC phase of compound **1** is thought to be a columnar phase.

In contrast, compound **2** exhibits a metastable columnar phase at room temperature. Over several days, this metastable columnar phase changed to another thermodynamically stable columnar phase. Figure 2(c) shows a polarizing optical micrograph of the metastable columnar phase of compound **2** at room temperature. Birefringent domains and relatively dark areas were observed. When the sample was rotated, the brightness of the birefringent domains changed, while the change in the transmittance of the dark areas was not remarkable (see supporting information). In the birefringent domains, the columnar aggregates could be aligned parallel to the substrate although the axes of the columnar aggregates are thought to be perpendicular to the substrate in the dark domains. Figure 2(d) shows a polarizing micrograph of the thermodynamically stable columnar phase. Because of the phase transition accompanied by the change of the lattice symmetry, defect lines were produced.

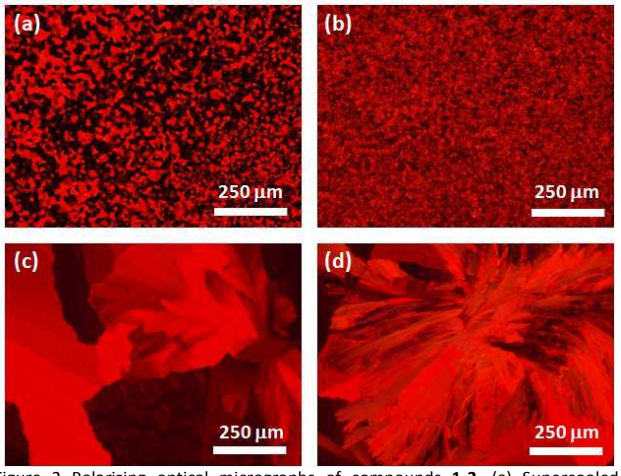

Figure 2 Polarizing optical micrographs of compounds **1**-**2**. (a) Supercooled columnar phase of compound **1** at room temperature. (b) Crystallization of compound **1** at room temperature. (c) Metastable columnar phase of compound **2** at room temperature. (d) Thermodynamically stable columnar phase of compound **2** at room temperature.

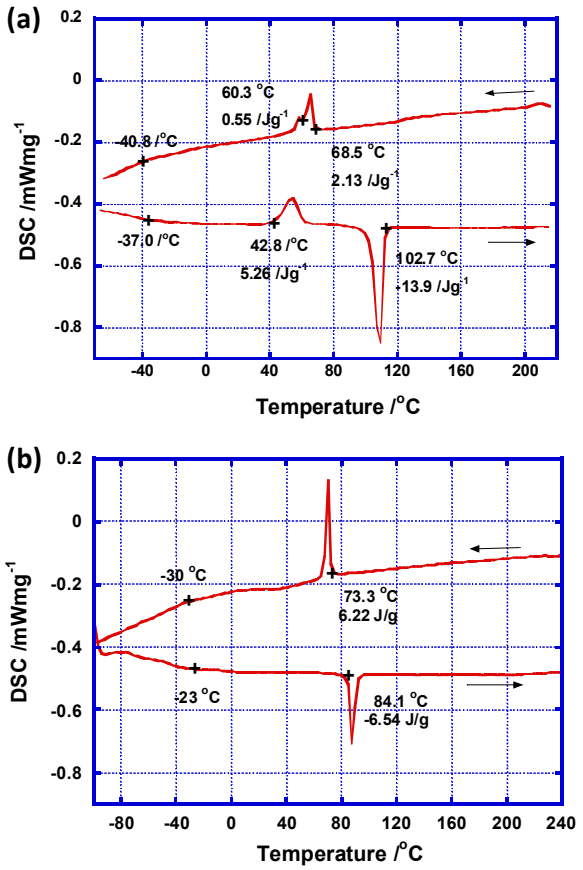

Figure 3 DSC thermograms of (a) compound **1** and (b) compound **2**. Heating/cooling rate: 10 Kmin^{-1}.

Figure 3 shows DSC thermograms of compounds **1**-**2**. Compound **1** formed a supercooled mesophase below 60.3 ºC. Around -40 ºC, the mesophase changed to a glassy mesophase. On heating, the glassy mesophase crystallized at 43 ºC, and melted to form an isotropic liquid at 102.7 ºC, indicating that the mesophase was metastable.

Only one peak was observed in the heating and cooling thermograms of compound **2**. The peak at 84.1 ºC in the heating curve and that at 73.3 ºC in the cooling curve indicate a transition from the metastable columnar phase to an isotropic liquid. The metastable columnar phase was stable within the time range of the DSC measurements. Glass transition based on freezing of the thermal motion of the cyclotetrasiloxane rings was observed around -30 ºC. No peaks derived from crystallization were observed during the heating and cooling processes.

Compared to the clearing point of 81 ºC for a previously reported sample containing a small amount of isomeric impurity,[11d] the clearing point of the present sample increased to 84 ºC during the heating process. The supercooling tendency was suppressed in the purified sample.

The mesophase of compound **1** is metastable and could not be characterized by X-ray diffraction when capillary tube samples were used. However, the metastable columnar phase of compound **2** could be characterized by X-ray diffraction given that the transition from the metastable columnar phase to the thermodynamically stable phase took several days. Figure 4(a) shows the X-ray diffraction pattern of the metastable columnar phase of compound **2** at room temperature. The strong diffraction peak at 2θ = 3.30º is assigned to the (100) diffraction plane with a lattice spacing of 26.8 Å. Assuming a hexagonal lattice, the other peaks at 2θ = 5.72º, 6.34º, 9.59º, 11.40º, and 12.28º were indexed to the (110), (200), (300), (220), and (310) diffraction planes, respectively. Between 9º and 13º, the diffraction peaks were superimposed on a broad halo originating from liquid-like packing of the cyclotetrasiloxane moieties. Such a broad halo is usually observed for the columnar phases of PTCBI and triphenylene derivatives bearing oligosiloxane chains.[4n] The broad halo around 20º is ascribed to liquid-like packing of the alkyl chains. No diffraction peak corresponding to the π-π stacking distance in the columnar aggregates was observed in the wide-angle region. Thus, this metastable columnar phase is identified to be a hexagonal columnar disordered phase.

Figure 4(b) shows the X-ray diffraction pattern of the thermodynamically stable columnar phase of compound **2**. A strong diffraction peak is observed at 2θ = 3.34º in the XRD profile of the mesophase of compound **2**, which is assigned to a (200) diffraction plane. This peak is accompanied by a peak at 2θ = 4.04º, which is derived from the (110) diffraction plane. Assuming a rectangular columnar arrangement with *P2m* symmetry with lattice constants of 52.8 and 24.0 Å, the other diffraction peaks observed at 2θ = 5.32º, 6.56º, 8.05º, 10.40º, 11.13º, 12.06º, 13.11º, 13.90º, 14.83º, 15.97º, 17.29º, 18.30º, 19.14º, 19.98º, 20.77º, 22.30º, and 23.50º were indexed to the (300), (400), (220), (600), (030), (330), (430), (530), (040), (730), (830), (050), (350), (450), (550), (060), and (460) diffraction planes, respectively. Between 9º and 13º, the diffraction peaks were superimposed on a broad halo originating from liquid-like aggregation of the cyclotetrasiloxane rings. Around 22º, the diffraction peaks were also superimposed on a halo derived from liquid-like packing of the alkyl chains.

No diffraction peak indicative of intracolumnar order was observed in the wide-angle region. Therefore, this phase is identified as a rectangular disordered columnar phase.

In the metastable columnar phase, the intercolumnar distance is around 30 Å, as deduced from the lattice constant of the (100) diffraction plane, which is much smaller than the extended molecular length of 52 Å (the latter was determined by optimization of the molecular structure using molecular mechanics calculation). This result indicates interdigitation of the cyclotetrasiloxane rings.

On the other hand, for the thermodynamically stable columnar phase, the lattice constant corresponding to the intercolumnar distance is 52.7 Å, which is comparable to the extended molecular length of 52 Å. The other lattice constant of 24 Å is shorter than the molecular length, indicating that the molecules are tilted within the columnar aggregates. In this columnar phase, the cyclotetrasiloxane rings do not interdigitate, in contrast with the remarkable interdigitation of the cyclotetrasiloxane rings in the metastable columnar phase. This is also different from the columnar phases of PTCBI derivatives

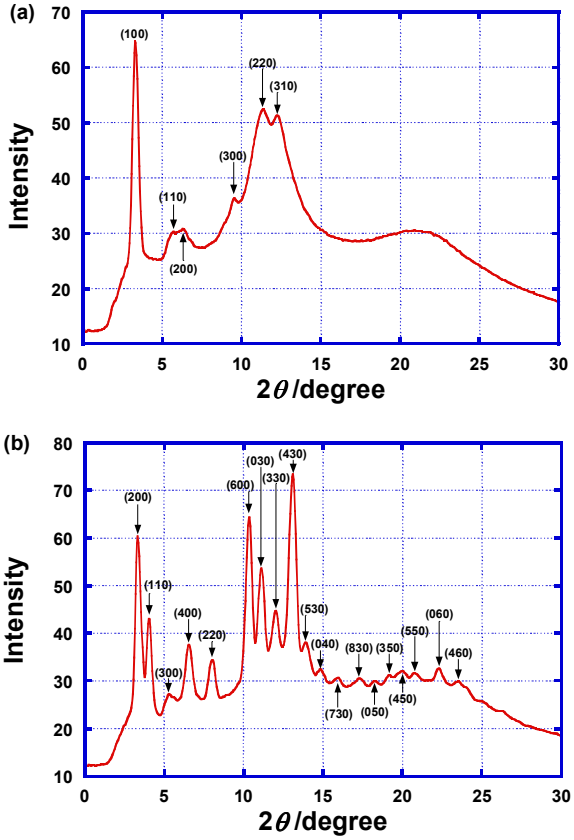

Figure 4 X-ray diffraction patterns of (a) metastable columnar phase and (b) thermodynamically stable columnar phase of compound **2** at room temperature.

bearing linear oligosiloxane chains, in which remarkable interdigitation of the oligosiloxane chains is observed.[11a-c]

Compared to the sample contaminated with an isomeric impurity, this purified sample exhibited the same rectangular columnar disordered phase. However, the lattice constant of the purified sample was different from that of the impure congener.[11d]

Carrier transport characteristics in the columnar phases of compounds 1-2

Figure 5(a) shows the transient photocurrent curves for the electrons in the metastable columnar phase of compound **2** at room temperature, using a cell with the thickness of 25 μm. Non-dispersive transient photocurrent curves were obtained between 20 ºC and 70 ºC. The electron mobility exceeded 1 × 10^{-1} $cm^2V^{-1}s^{-1}$ at room temperature. In the temperature range of 20–70 ºC, the electron mobility was independent of the temperature and electric field (Figure 5(b)). This result is quite different from the behavior of organic amorphous semiconductors and indicates small energetic and positional disorders in the columnar phase.[11e]

For compound **2**, the room temperature electron mobility in the columnar phase of the sample containing the isomeric impurity was 1 × 10^{-2} $cm^2V^{-1}s^{-1}$.[11b] Removal of the impurity increased the electron mobility by a factor of 10. This electron mobility exceeding 1 × 10^{-1} $cm^2V^{-1}s^{-1}$ is the highest value reported for columnar liquid crystals to date. We previously reported high electron mobility of the order of 10^{-1} $cm^2V^{-1}s^{-1}$ for the ordered columnar phase of a PTCBI derivative bearing four disiloxane chains at the terminals of the alkyl side chains.[11b] The ordered columnar phase of the PTCBI derivatives is characterized by close π-π stacking and periodical order of the molecular position within the columnar aggregates. In contrast, compound **2** has four bulky cyclotetrasiloxane rings and consequently forms the disordered columnar phase in which there is no periodicity of the molecular position within the columnar aggregates.

In the thermodynamically stable rectangular columnar phase of compound **2**, only dispersive transient photocurrent curves were obtained for the electrons and the electron mobility could not be determined. The defects produced during the transition from the hexagonal to rectangular phase may affect the electron transport.

For compound **1**, TOF measurement of the metastable columnar phase in a LC cell was possible only within a limited time span. At room temperature, non-dispersive transient photocurrent curves were obtained for electrons in the metastable columnar phase. The electron mobility was 1 × 10^{-2} $cm^2V^{-1}s^{-1}$, determined by the TOF measurement using a cell with the thickness of 25 μm. After allowing the sample to stand at room temperature for 30 min, the transient photocurrent curves changed to weak featureless decay curves because of crystallization of the sample and the consequent formation of defects.

Only very weak current decays were observed for holes in the columnar phase of these compounds, and the hole mobilities could not be determined.

Structures of spin-coated and polymerized LC thin films of compound 2

Compound **2** can be polymerized in the solution state. In the presence of a catalytic amount of trifluoromethane sulfonic acid, gel-like precipitates were produced in the dichloromethane solution of compound **2**. The obtained precipitates were insoluble in organic solvents such as dichloromethane, chloroform, tetrahydrofuran, and toluene. Compound **2** has four reactive groups and an insoluble network polymer could be formed in the solution state. Thin films of the polymerized compound **2** could not be produced using the precipitates formed in the solution state.

Compound **2** was soluble in various organic solvents, except for alcohols, and LC thin films could be produced by the spin-coating method. However, the deposited thin films of compound **2** dissolved in organic solvents. After exposure of the thin films to trifluoromethane sulfonic acid vapor, the spin-coated thin films became insoluble in various organic solvents such as dichloromethane, chloroform, tetrahydrofuran, acetone, and toluene.

Figure 6 shows DSC thermograms of the polymerized thin film. The peaks corresponding to the phase transition between the isotropic and columnar phases in the heating as well as cooling processes completely disappeared in the profile of the polymerized thin film. This indicates the formation of polysiloxane networks during exposure to the acid vapor.

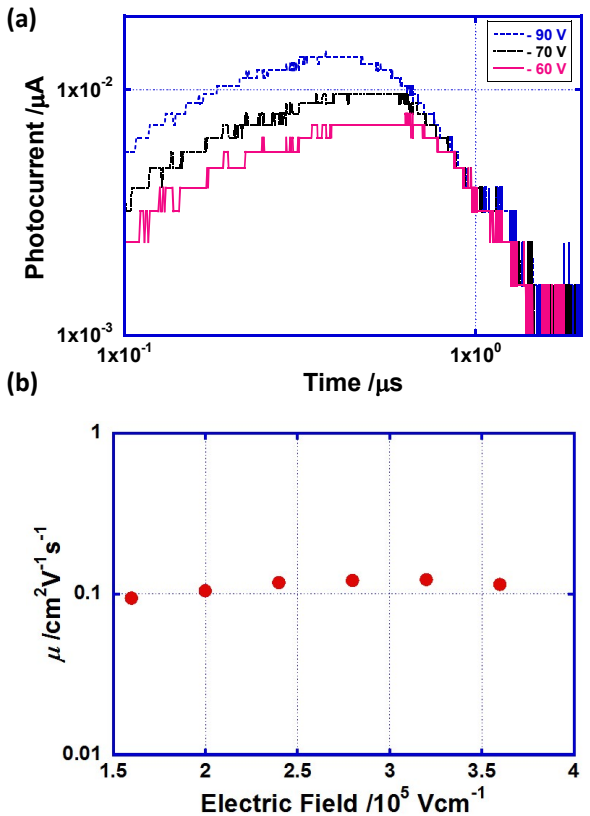

Figure 5 (a) Transient photocurrent curves for electrons in the ordered columnar phase of compound **2** at room temperature. The sample thickness was 25 μm and the wavelength of the excitation light was 256 nm. (b) The electron mobility at room temperature as a function of the electric field.

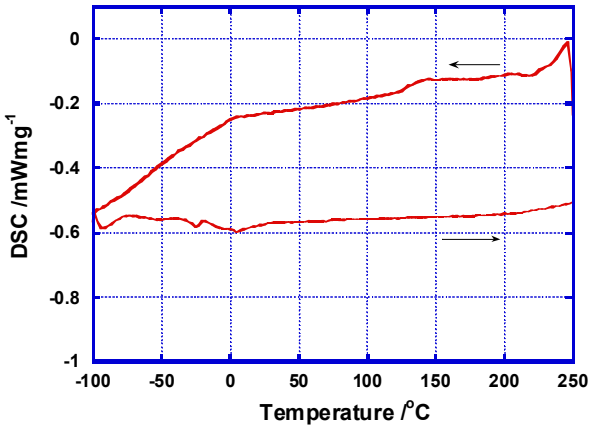

Figure 6 DSC thermograms of polymerized thin film of compound **2**. Heating/cooling rate: 10 Kmin^{-1}.

During exposure to the acid vapor, the four reactive cyclotetrasiloxane rings could polymerize to form a network polymer via the acid-catalyzed ring-opening mechanism. Figure 7 shows the IR-absorption spectra of the as-deposited and polymerized thin films of compound **2**. The spectra of the monomeric and the polymeric thin films were almost the same, except for the broad peak at 1100–1200 cm^{-1} that was assigned to the Si-O stretching vibration. The absorption band at 1100–1200 cm^{-1}in the spectrum of the polymerized thin film was broader than that of the as-deposited thin film. This should be attributed to restriction of the thermal motion of the cyclotetrasiloxane rings in the as-deposited thin films. Polydispersity of the polymerization and structural disorder of the polymerized thin films should also affect the broadening of the peak. The peaks between 1200 and 1800 cm^{-1}, which were derived from the PTCBI core, did not change remarkably during the polymerization process. This result indicates that the cyclotetrasiloxane moieties polymerized to form a network polymer without degradation of the PTCBI core upon exposure to the acid vapor.

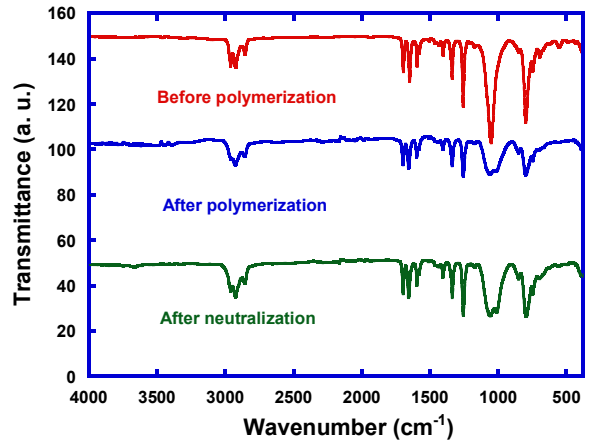

Figure 7 IR transmission spectra of the as-deposited, polymerized, and neutralized thin films of compound **2**.

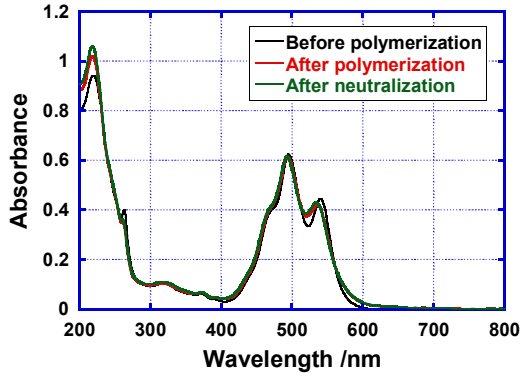

Figure 8 UV-Vis absorption spectra of as-deposited and polymerized thin films of compound **2**.

Figure 8 shows the UV-Vis absorption spectra of the as-deposited and polymerized thin films with a thickness of 500 nm. The absorption peak at 494 nm and the shoulder at 470 nm did not change during the polymerization and neutralization processes, whereas the peak at 540 nm underwent a slight hypsochromic shift to 535 nm. The absorption spectrum of the thin film after the neutralization process was almost the same as the original spectrum prior to polymerization. The slight blue shift and broadening of the absorption peak in the case of the thin film should be attributed to an increase in the structural disorder in the polymerized thin film.

For thicker films (thickness > 1 μm), there was a remarkable color change after exposure to the trifluoromethane sulfonic acid vapor. The color of the film changed from red to purple during the polymerization process. The red color of the thin films was regained upon neutralization.

The domain structures of the as-deposited thin films were retained during polymerization. Figure 9 presents the polarizing optical micrographs of the thin films of compound **2**. Figure 9(a) corresponds to the thin films annealed at 80 ºC for 1 h prior to polymerization. Before the thermal treatment, the thin film consisted of small domains whose sizes were less than 1 μm.

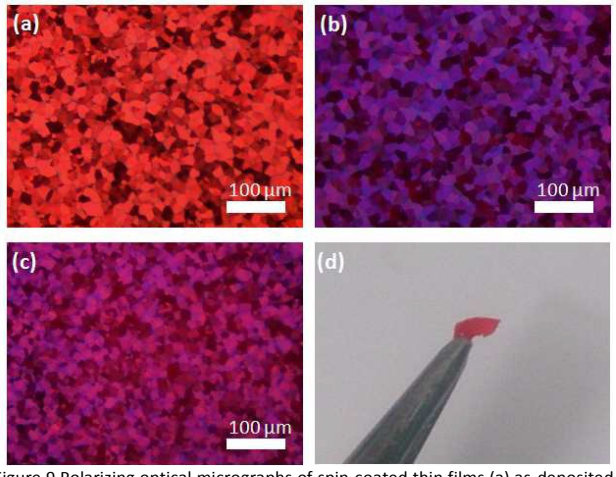

Figure 9 Polarizing optical micrographs of spin-coated thin films (a) as-deposited, (b) after exposure to the acid vapor, and (c) after neutralization with triethylamine. (d) Photograph of polymerized thin film peeled from the substrate.

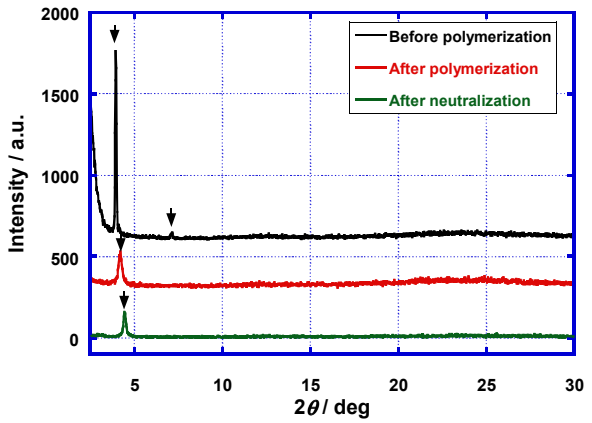

Figure 10 X-ray diffraction patterns of spin-coated thin films before and after polymerization by exposure to trifluoromethane sulfonic acid vapor. Arrows indicates diffraction peaks.

After the thermal annealing, domains with dimensions of several tens of micrometers were formed. These domains were birefringent and their transmittances changed upon rotation through a 180° angle, indicating that the columnar aggregates aligned uniaxially within the domains and the columnar axes were parallel to the substrate in the domains. Figure 9(b) corresponds to the thin film after exposure to trifluoromethane sulfonic acid vapor at 80 ºC for 30 min. The birefringence and size of the domains were retained during the polymerization process. Protonation of the aromatic cores should induce a color change of the thin films to purple. Figure 9(c) shows the polarizing optical texture of the thin film after neutralization in a triethylamine solution. The purple color changed to red, but the color of the thin film was not completely regained. This should be attributed to the slight change of the molecular aggregation state after the polymerization. The domain size and birefringence were also retained after neutralization.

As shown in Figure 9(d), the polymerized thin films could be peeled off the substrates to produce self-standing films. The self-standing films could be bent. Compound **2** has four reactive groups, and an element-block type polysiloxane network[15] is formed during polymerization. The insolubility and mechanical stability of the thin films should be derived from the polymer network.

X-ray diffraction patterns in the thin film state for the spin-coated thin film of compound **2** are presented in Figure 10. Before polymerization, two peaks were apparent at $2\theta = 3.94°$ and 7.14º in the diffraction pattern; the corresponding lattice

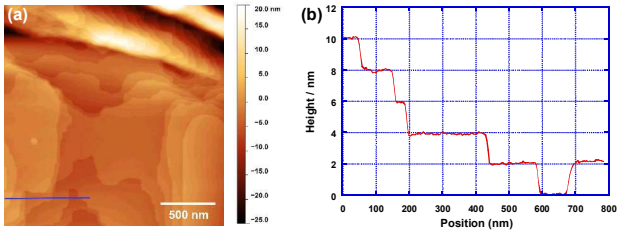

Figure 11 (a) AFM observation of the surface morphology of the spin-coated LC thin films. (b) Surface profile of the LC thin film along the blue line in (a).

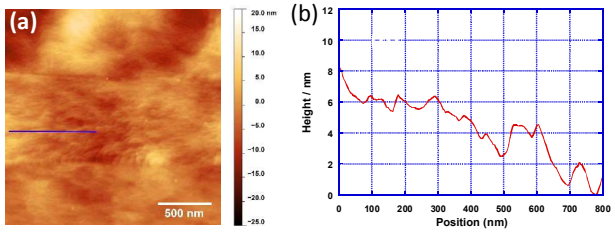

Figure 12 (a) AFM observation of the surface morphology of the polymerized LC thin films. (b) Surface profile of the polymerized thin film along the blue line in (a).

constants are 22.4 Å and 12.8 Å. The ratio of the lattice constants is √3, indicating hexagonal columnar order in the thin film state. The strong peak in the profile of the thin film shifted to a higher angle compared to the strongest diffraction peak in the profile of the bulk phase of compound **2**. The molecular aggregation structure in the thin film state may differ from that of the bulk LC phase.

After polymerization, one diffraction peak was observed in the thin film state. The peak was broadened and shifted to $2\theta =$ 4.2º, indicating that structural disorder was induced and the two-dimensional lattice shrank during the polymerization process. The diffraction peak shifted to 4.4º and the lattice constant became smaller after the neutralization process.

The surface morphology of the as-deposited LC films and polymerized LC films was studied by AFM. Figure 11(a) displays the height images of the as-deposited films. Terrace structures were observed on the surface of the spin-coated films. Figure 11(b) indicates the surface profile of the LC thin film. The height of the steps was around 24 Å, which is comparable to the diameter of the columnar aggregates, 22.4 Å, determined from X-ray diffraction, as shown in Figure 10. The observed terrace structure may be attributed to the hexagonal columnar organization in which the columnar aggregates align parallel to the substrate in the thin film.

For the polymerized thin films, the homogeneous terrace structure was partially broken and a fibrous structure was observed, as shown in Figure 12. The root mean square (RMS) surface roughness of both terrace structures increased from 1.4 Å to 6 Å during the polymerization process. This observation indicates an increase in the structural disorder during the polymerization process and is consistent with the X-ray diffraction analysis. During polymerization, the positional change of the siloxane moieties at the ends of the side chains could induce distortion of the columnar aggregates and the terrace structures.

In contrast to compound **2**, thin films of compound **1** produced by the spin-coating method immediately crystallized and homogeneous thin films of compound **1** could not be obtained. The crystallized thin films of compound **2** did not polymerize under the same condition.

Uniaxially aligned thin film of compound 2

Control of the orientation of the columnar aggregates is desirable for the application of the columnar LC semicondcutors in optical and electronic devices. Spin-coated thin films on non-treated substrates consist of LC domains with sizes of several tens of micrometers, as shown in Figure 9. The

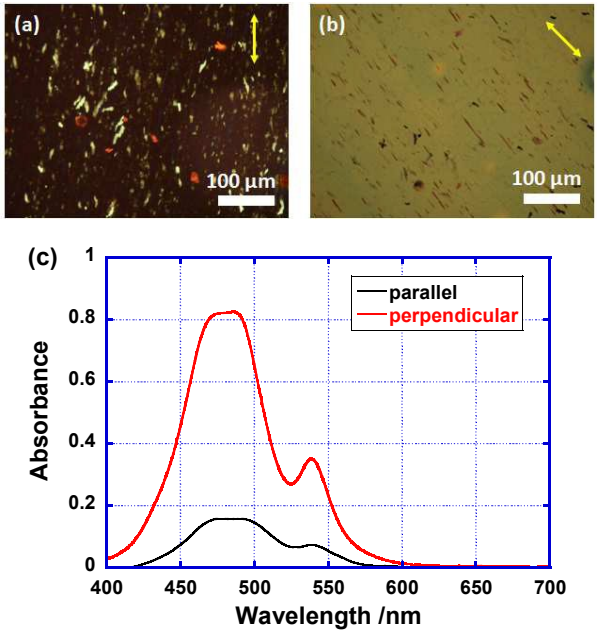

Figure 13 Polarizing optical micrographs of a uniaxially aligned spin-coated film of compound **2**. The optical axis of the polarizer was (a) parallel to the direction of the friction and (b) tilted by 45° to the direction. The yellow arrow indicates the direction of the friction. (c) Polarized absorption spectra of the thin film.

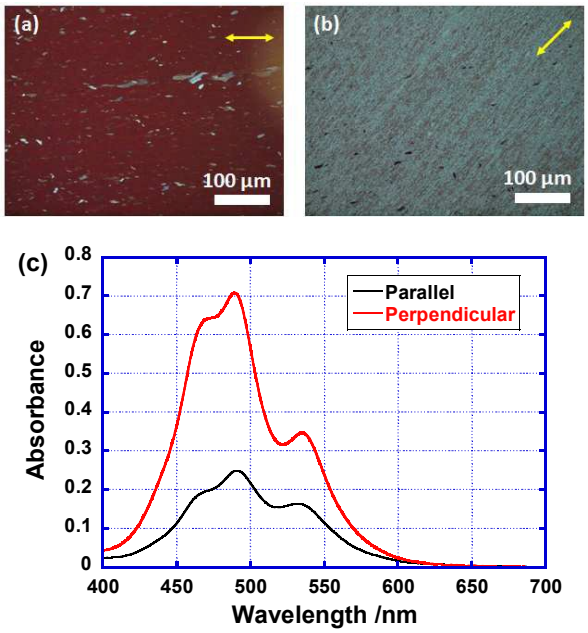

Figure 14 Polarized absorption spectra of the thin film of compound **2** after polymerization and neutralization. The optical axis of the polarizer was (a) parallel to the direction of the friction and (b) tilted by 45° to the direction. The yellow arrow indicates the direction of the friction. (c) Polarized absorption spectra of the thin film.

columnar axes of the domains were parallel to the substrates and oriented randomly.

In contrast, a uniaxially aligned thin film could be produced on friction transferred[16] substrates by the spin-coating method. In the friction transfer method, the surface of a substrate that was heated to over 220 ºC was rubbed with a block of Teflon. Teflon fibers aligned in the direction of the friction adhered to the surface. Formation of a uniaxially aligned film of columnar phases of hexabenzocoronene and PTCBI derivatives has already been reported.[7c, 11b]

Figure 13(a)-(b) shows polarizing optical micrographs of a spin-coated film of compound **2** on a friction transferred glass substrate. The transmittance changed periodically depending on the angle between the columnar axis and the optical axis of the polarizer. This indicates that a macroscopically aligned film with a size exceeding several hundreds of micrometers was formed. Figure 13(c) shows polarized absorption spectra of the uniaxially aligned thin film. The dichroic ratio at 480 nm was 5.3:1. The light polarized vertical to the friction direction was absorbed to a greater extent than that parallel to the direction. The columnar aggregates could be aligned along the Teflon fibers and the columnar axis was consistent with the friction direction. The transition moments of the PTCBI cores are restricted within the π-conjugated plane and the light polarized vertical to the friction direction could be more strongly absorbed. The uniaxially aligned thin films were also polymerized by exposure to trifluoromethanesulfonic acid vapor, with retention of the molecular alignment.

Figure 14 shows polarizing optical micrographs and polarized absorption spectra of the polymerized thin films. As shown in Figure 14(a) and (b), the optical uniaxiality and defect density of the thin film were maintained during polymerization. The dichroic ratio, determined from the polarized absorption spectra, decreased to 2.8:1, as shown in Figure 14(c). This result is consistent with the X-ray diffraction patterns of the polymerized thin films.

The characterization of the electron transport in the polymerized thin films is in progress. In conventional TOF measurement using sandwich LC cells, homeotropically aligned films with the thickness of several µm are necessary because the electron transport is anisotropic in the columnar phases and the columnar axis has to be parallel to the electric field. However, the columnar aggregates aligned parallel to the substrate surface in the spin-coated thin films. The production of the polymerized thin films in which the columnar aggregates align perpendicular to the electrode surface by the spin-coating method has not been successful. The control of the columnar orientation in the spin-coated thin films is in progress.

Comparison with related system

Polymerization of smectic and columnar LCs in the solution state has been carried out by radical and metathesis reactions.[17] However, it is difficult to produce macroscopically aligned thin films from solution-synthesized LC polymers exhibiting smectic and columnar phases.

In-situ polymerization in the thin film state using photo-initiators is effective for generating macroscopically aligned LC films. In addition to photopolymerization of nematic LC films,[12] *in-situ* photopolymerization of π-conjugated LC semiconductor molecules bearing acrylate groups and oxetane moieties in ordered smectic phases has also been reported.[13] *In-situ* polymerization of columnar LC molecules based on triphenylene units was also attempted.[14] However,

macroscopically aligned thin films were not successfully generated.

Conventional photoactive radical initiators and acid generators are active upon deep UV irradiation. Acid generators and radical initiators that are active upon deep UV irradiation are effective for the photopolymerization of ion-conductive LC molecules based on small π-conjugated systems.[18] LC molecules based on extended π-conjugated systems absorb strongly in the deep UV region, and therefore, radical-initiated or acid-catalyzed photopolymerization cannot be applied to LC semiconductors. The acid-vapor-catalyzed *in-situ* polymerization method for the LC thin films developed herein can be applied to LC semiconductors possessing extended π-conjugated systems.

In addition to the friction transfer method,[7c,11b] zone-cast and sharing methods have been used for the production of uniaxially aligned thin films of columnar LCs.[7d,9c,17a] Insolubilization of the uniaxially aligned thin films of columnar LCs has not yet been reported. The acid-vapor-catalyzed *in-situ* polymerization described herein facilitates the formation of self-standing thin films as well as insoluble optically anisotropic LC thin films.

Conclusions

The perylene tetracarboxylic bisimide (PTCBI) derivative bearing four cyclotetrasiloxane rings presented herein forms a columnar phase at room temperature, in spite of the presence of the bulky cyclotetrasiloxane rings. This columnar phase has an electron mobility of 0.12 $cm^2V^{-1}s^{-1}$ at room temperature. Thin films of compound **2** deposited by the spin-coating method were insolubilized by exposure to trifluoromethane sulfonic acid vapor. Ring-opening polymerization catalyzed by the acid vapor produced a polymer network with an element-block structure and the columnar LC structure was retained. Uniaxially aligned LC thin films were successfully produced by the friction transfer method. The optical anisotropy of the thin films was also retained during the polymerization process. Further study on the carrier transport properties of the polymerized thin films is in progress.

Acknowledgements

This study was financially supported by the Japan Security Scholarship Foundation, the Ogasawara Foundation, a Grant-in-Aid for Scientific Research on Innovative Areas (Coordination Programming, no. 24108729 and Element-Block Polymers, no. 25102533) from the Ministry of Education, Culture, Sports, Science, and Technology (MEXT), a Grant-in-Aid for Scientific Research (B) (no. 22350080) from the Japan Society for the Promotion of Science (JSPS), the Iwatani Naoji Foundation, the Asahi Glass Foundation, the Murata Science Foundation, and the TEPCO Memorial Foundation. The authors thank Dr. A. Sonoda at Health Research Institute, National Institute of Advanced Industrial Science and Technology for help with the NMR measurements. The authors also thank Prof. T. Ishii and Prof. T. Kusunose at Kagawa University for help with the X-ray diffraction and DSC measurements, respectively. Elemental analyses were carried out at the Engineering Research Equipment Centre of Kumamoto University and Sumika Chemical Analysis Service, Ltd.

Notes and references

1 (a) A. N. Sokolov, B. C.-K. Tee, C. J. Bettinger, J. B.-H. Tok, Z. Bao, *Acc. Chem. Res*., 2012, **45**, 361–371; (b) J. Rivnay, L. H. Jimison, J. E. Northrup, M. F. Toney, R. Noriega, S. Lu, T. J. Marks, A. Facchetti, A. Salleo, *Nat. Mater*., 2009, **8**, 952-958; (c) Y. Yuan, G. Giri, A. L. Ayzner, A. P. Zoombelt, S. C. B. Mannsfeld, J. Chen, D. Nordlund, M. F. Toney, J. Huang, Z. Bao, *Nat. Commun*., 2014, **5**, 3005; (d) J. E. Anthony, *Chem. Rev*., 2006, **106**, 5028–5048; (e) I. Osaka, R. D. McCullough, *Acc. Chem. Res*., 2008, **41**, 1202–1214.

2(a) Y.-H. Niu, M. S. Liu, J.-W. Ka, A. K.-Y. Jen, *Appl. Phys. Lett*., 2006, **88**, 093505; (b) Y. Shao, X. Gong, A. J. Heeger, M. Liu, A. K.-Y. Jen, *Adv. Mater*., 2009, **21**, 1972–1975; (d) G. Wantz, L. Derue, O. Dautel, A. Rivaton, P. Hudhommed, C. Dagron-Lartigau, *Polym. Int*., 2014, **63**, 1346–1361; (e) A. W. Hains, H.-Y. Chen, T. H. Reilly, III, B. A. Gregg, *ACS Appl. Mater. Interfaces*, 2011, **3**, 4381–4387; (f) N. Aizawa,Y. -J. Pu, M. Watanabe, T. Chiba,K. Ideta,N. Toyota,M. Igarashi,Y. Suzuri,H. Sasabe,J. Kido, *Nat. Commun*., 2014, **5**, 5756.

3 (a) W. Pisula, M. Zorn, J. Y. Chang, K. Müllen, R. Zentel, *Macromol. Rapid Commun*., 2009, **30**, 1179-1202; (b) Y. Shimizu, K. Oikawa, K. Nakayama, D. Guillon, *J. Mater. Chem*. 2007, **17**, 4223-4229. (c) M. O'Neill, S. M. Kelly, *Adv. Mater*., 2011, **23**, 566-584. (d) M. Funahashi, H. Shimura, M. Yoshio, T. Kato, *Structure and Bonding*, 2008, **128**, 151-179. (e) M. Funahashi, T. Yasuda, T. Kato, *Handbook of Liquid Crystals* 2nd Ed. Wiley-VCH, 2014, **8**, 675-708.

4 (a) D. Adam, F. Closs, T. Frey, D. Funhoff, D. Haarer, H. Ringsdorf, P. Schuhmacher, K. Siemensmeyer, *Phys. Rev. Lett*., 1993, **70**, 457–460; (b) D. Adam, P. Schumacher, J. Simmerer, L. Haussling, K. Siemensmeyer, K. H. Etzbach, H. Ringsdorf, D. Haarer, *Nature*, 1994, **371**, 141–143; (c) N. Boden, R. J. Bushby, J. Clements, B. Movaghar, K. J. Donovan, T. Kreouzis, *Phys. Rev. B*, 1995, **52**, 13274–13280. (d) A. M. van de Craats, J. M. Warman, A. Fechtenkötter, J. D. Brand, M. A. Harbison, K. Müllen, *Adv. Mater*., 1999, **11**, 1469–1472. (e) M. Ichihara, A. Suzuki, K. Hatsusaka, K. Ohta, *Liq. Cryst*., 2007, **34**, 555–567. (f) K. Ban, K. Nishikawa, K. Ohta, A. M. van de Craats, J. M. Warman, I. Yamamoto, H. Shirai, *J. Mater. Chem*., 2001, **11**, 321–331. (g) A. Demenev, S. H. Eichhorn, T. Taerum, D. Perepichka, S. Patwardhan, F. C. Grozema, L. D. A. Siebbeles, *Chem. Mater*., 2010, **22**, 1420-1428. (h) J. Simmerer, B. Glüsen, W. Paulus, A. Kettner, P. Schuhmacher, D. Adam, K.-H. Etzbach, K. Siemensmeyer, J. H. Wendorf, H. Ringsdorf, D. Haarer, *Adv. Mater*., 1996, **8**, 815-819; (i) F. Würthner, *Chem. Commun*., 2004, 1564–1579; (j) F. Würthner, C. Thalacker, S. Diele, C. Tschierske, *Chem. Eur. J*., 2001, **7**, 2245–2253. (k) Z. Chen, U. Baumeister, C. Tschierske, F. Würthner, *Chem. Eur. J*., 2007, **13**, 450–465. (l) A. Wicklein, M-A. Muth, M. Thelakkat, *J. Mater. Chem*., 2010, **20**, 8646-8652; (m) A. Wicklein, A. Lang, M. Muth, M. Thelakkat, *J. Am Chem. Soc*., 2009, **131**, 14442–14453; (n) A. Zelcer, B. Donnio, C. Bourgogne, F. D. Cukiernik, D. Guillon, *Chem. Mater*., 2007, **19**, 1992–2006.

5 (a) M. Funahashi, J. Hanna, *Phys. Rev. Lett*., 1997, **78**, 2184–2187. (b) M. Funahashi, J. Hanna, *Appl. Phys. Lett*., 2000, **76**, 2574–2576. (c) M. Funahashi, J. Hanna, *Adv. Mater*., 2005, **17**, 594–598. (d) K. Oikawa, H. Monobe, J. Takahashi, K. Tsuchiya, B. Heinrich, D. Guillon, Y. Shimizu, *Chem. Commun*.,

2005, 5337–5339. (e) A. Matsui, M. Funahashi, T. Tsuji, T. Kato, *Chem. Eur. J*., 2010, **16**, 13465–13472. (f) H. Aboubakr, M.-G. Tamba, A. K. Diallo, C. Videlot-Ackermann, L. Belec, O. Siri, J.-M. Raimundo, G. H. Mehl, H. Brisset, *J. Mater. Chem*., 2012, **22**, 23159–23168. (g) M. Funahashi, F. Zhang, N. Tamaoki, J. Hanna, *ChemPhysChem*, 2008, **9**, 1465–1473. (h) M. Funahashi, T. Ishii, A. Sonoda, *ChemPhysChem*, 2013, **14**, 2750–2758.

6 (a) T. Hassheider, S. A. Benning, H.-S. Kitzerow, M.-F. Achard, H. Bock, *Angew. Chem., Int. Ed*., 2001, **40**, 2060–2063. (b) M. P. Aldred, A. E. A. Contoret, S. R. Farrar, S. M. Kelly, D. Mathieson, M. O'Neill, W. C. Tsoi, P. Vlachos, *Adv. Mater*., 2005, **17**, 1368–1372. (c) S. A. Benning, R. Oesterhaus, H.-S. Kitzerow, *Liq. Cryst*., 2004, **31**, 201–205.

7 (a) A. J. J. M. van Breemen, P. T. Herwig, C. H. T. Chlon, J. Sweelssen, H. F. M. Schoo, S. Setayesh, W. M. Hardeman, C. A. Martin, D. M. de Leeuw, J. J. P. Valeton, C. W. M. Bastiaansen, D. J. Broer, A. R. Popa-Merticaru, S. C. J. Meskers, *J. Am. Chem. Soc*., 2006, **128**, 2336–2345. (b) M. Funahashi, F. Zhang, N. Tamaoki, *Adv. Mater*., 2007, **19**, 353–358. (c) A. M. van de Craats, N. Stutzmann, O. Bunk, M. M. Nielsen, M. Watson, K. Müllen, H. D. Chanzy, H. Sirringhaus, R. Friend, Adv. Mater., 2003, **15**, 495–499; (d) W. Pisula, A. Menon, M. Stepputat, I. Lieberwirth, U. Kolb, A. Tracz, H. Sirringhaus, T. Pakula, K. Müllen, *Adv. Mater*., 2005, **17**, 684–689. (e) M. Funahashi, *Polym. J*., 2009, **41**, 459–469. (f) F. Zhang, M. Funahashi, N. Tamaoki, *Org. Electr*., 2010, **11**, 363–368.

8 (a) L. Schmidt-Mende, A. Fechtenkötter, K. Müllen, E. Moons, R. H. Friend, J. D. MacKenzie, *Science*, 2001, **293**, 1119–1122; (b) T. Hori, Y. Miyake, N. Yamasaki, H. Yoshida, A. Fujii, Y. Shimizu, M. Ozaki, *Appl. Phys. Exp*., 2010, **3**, 101602. (c) W. Shin, T. Yasuda, G. Watanabe, Y. S. Yang, C. Adachi, *Chem. Mater*., 2013, **25**, 2549–2556. (d) K. Sun, Z. Xiao, S. Lu, W. Zajaczkowski, W. Pisula, E. Hanssen, J. M. White, R. M. Williamson, J. Subbiah, J. Ouyang, A. B. Holmes, W. W. H. Wong, D. J. Jones, *Nat. Commun*., 2015, **6**, 6013.

9 (a) T. Kato, T. Yasuda, Y. Kamikawa, M. Yoshio, *Chem. Commun*., 2009, 729–739. (b) A. Matsui, M. Funahashi, T. Tsuji, T. Kato, *Chem. Eur. J*., 2010, **16**, 13465–13472; (c) T. Yasuda, H. Ooi, J. Morita, Y. Akama, K. Minoura, M. Funahashi, T. Shimomura, T. Kato, *Adv. Funct. Mater*., 2009, **19**, 411–419. (d) S. Yazaki, M. Funahashi, T. Kato, *J. Am. Chem. Soc*., 2008, **130**, 13206–13207. (e) S. Yazaki, M. Funahashi, J. Kagimoto, H. Ohno, T. Kato, *J. Am. Chem. Soc*., 2010, **132**, 7702–7708. (e) M. Yoneya, *Chem. Rec*., 2011, **11**, 66–76. (f) A. Seki, M. Funahashi, *Heterocycles*, 2015, in press.

10 (a) F. Würthner, C. R. Saha-Möller, B. Fimmel, S. Ogi, P. Leowanawat, D. Schmidt, *Chem. Rev*., 2015, **115**, in press; (b) H. Langhals, *Helv. Chim. Acta*, 2005, **88**, 1309-1343; (c) M. Funahashi, *J. Mater. Chem. C*, 2014, **2**, 7451–7459.

11 (a) M. Funahashi, A. Sonoda, *Org. Electr*., 2012, **13**, 1633–1640; (b) M. Funahashi, A. Sonoda, *J. Mater. Chem*., 2012, **22**, 25190–25197; (c) M. Funahashi, A. Sonoda, *Dalton Trans*., 2013, **42**, 15987–15994; (d) M. Funahashi, M. Yamaoka, K. Takenami, A. Sonoda, *J. Mater. Chem. C*, 2013, **1**, 7872–7878; (e) M. Funahashi, T. Ishii, A. Sonoda, *Phys. Chem. Chem. Phys*., 2014, **16**, 7754–7763.

12 (a) A. E. A. Contoret, S. R. Farrar, M. O'Neill, J. E. Nicholls, G. J. Richards, S. M. Kelly, A. W. Hall, *Chem. Mater*., 2002, **14**, 1477–1487; (b) A. E. A. Contoret, S. R. Farrar, P. O. Jackson, S. M. Khan, L. May, M. O'Neill, J. E. Nicholls, S. M. Kelly, G. J. Richards, *Adv. Mater*., 2000, **12**, 971–974; (c) P. Vlachos, S. M. Kelly, B. Mansoor, M. O'Neill, *Chem. Commun*., **2002**, 874–875.

13 (a) T. Kreouzis, B. J. Baldwin, M. Shkunov, I. McCulloch, M. Heeney, and W. Zhang, *Appl. Phys. Lett*., 2005, **87**, 172110; (b) I. McCulloch, C. Bailey, K. Genevicius, M. Heeney, M. Shkunov, D. Sparrowe, S. Tierney, W. Zhang, R. Baldwin, T. Kreouzis, J. W. Andreasen, D. W. Breiby, and M. M. Nielsen, *Phil. Trans. R. Soc. A*, 2006, **364**, 2779–2787; (c) I. McCulloch, M. Coelle, K. Genevicius, R. Hamilton, M. Heckmeier, M. Heeney, T. Kreouzis, M. Shkunov, and W. Zhang, *Jpn. J. Appl. Phys*., 2008, **47**, 488–491; (d) B.-H. Huisman, J.J.P. Valeton, W. Nijssen, J. Lub, W. ten Hoeve, *Adv. Mater*., 2003, **15**, 2002–2005; (e) I. McCulloch, W. Zhang, M. Heeney, C. Bailey, M. Giles, D. Graham, M. Shkunov, D. Sparrowe, and S. Tierney, *J. Mater. Chem*., 2003, **13**, 2436–2444.

14 (a) I. Bleyl, C. Erdelen, K.-H. Etzbach, W. Paulus, H.-W. Schmidt, K. Siemensmeyer, and D. Haarer, *Mol. Cryst. Liq. Cryst*., 1997, **299**, 149–155; (b) M. Inoue, H. Monobe, M. Ukon, V. F. Petrov, T. Watanabe, A. Kumano, and Y. Shimizu, *Opto-electronics Rev*., 2005, **13**, 303–308; (c) D.-G. Kang, D.-Y. Kim, M. Park, Y.-J. Choi, P. Im, J.-H. Lee, S.-W. Kang, and K.-U. Jeong, *Macromolecules*, 2015, **48**, 898–907.

15 Y. Chujo, K. Tanaka, *Bull. Chem. Soc. Jpn*., 2015, **88**, 633–643.

16 (a) J. C. Wittmann and P. Smith, *Nature*, 1991, **352**, 414–416; (b)Y. Ueda, T. Kuriyama, T. Hari, M. Watanabe, N. Jinping, Y. Hattori, N. Uenishi, and T. Uemiya, *Jpn. J. Appl. Phys.*, 1995, **34**, 3876–3883; (c) Y. Hosokawa, M. Misaki, S. Yamamoto, M. Torii, K. Ishida, Y. Ueda, *Appl. Phys. Lett*., 2012, **100**, 203305.

17 (a) M. Weck, B. Mohr, B. R. Maughon, and R. H. Grubbs, *Macromolecules*, 1997, **30**, 6430–6437; (b) Y.-F. Zhu, X.-L. Guan, Z. Shen, X.-H. Fan, and Q.-F. Zhou, *Macromolecules*, 2012, **45**, 3346–3355.

18 (a) M. Yoshio, T. Kagata, K. Hoshino, T. Mukai, H. Ohno, T. Kato, *J. Am. Chem. Soc*., 2006, **128**, 5570–5577; (b) Y. Ishida, H. Sakata, A. S. Achalkumar, K. Yamada, Y. Matsuoka, N. Iwahashi, S. Amano, and K. Saigo, *Chem. Eur. J*., 2011, **17**, 14752–14762.

Table of Contents

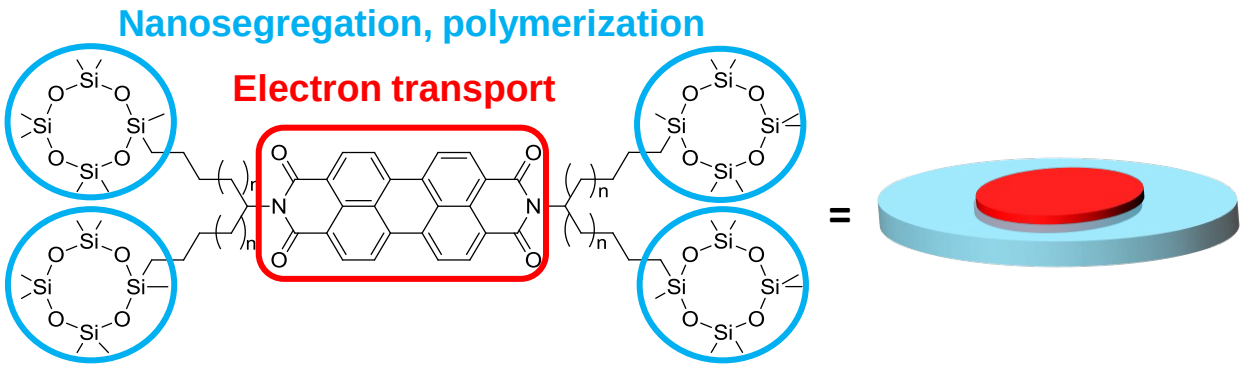

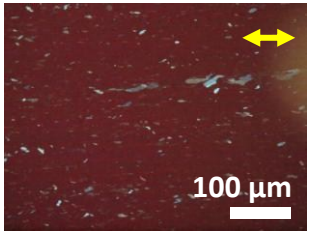

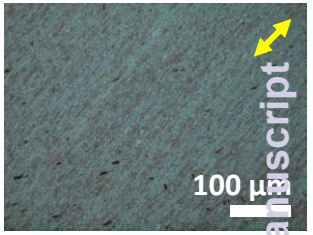

Uniaxially aligned thin film

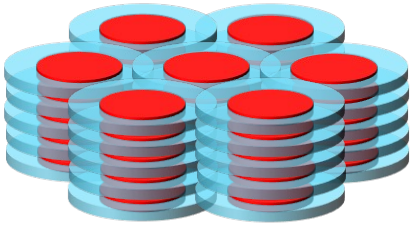

CF_3SO_3H vapor

In situ ring-opening polymerization

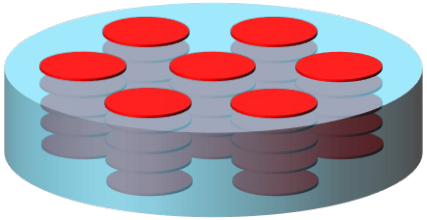

Self-standing film